

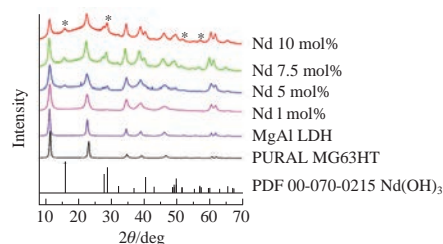
Induced neodymium luminescence in sol–gel derived layered double hydroxides

 Aurelija Smalenskaite,^a Andrei N. Salak^b and Aivaras Kareiva^{*a}
^a Department of Inorganic Chemistry, Institute of Chemistry, Vilnius University, LT-03225 Vilnius, Lithuania.
E-mail: aivaras.kareiva@chgf.vu.lt

^b Department of Materials and Ceramic Engineering and CICECO, Aveiro Institute of Materials, 3810-193 Aveiro, Portugal

DOI: 10.1016/j.mencom.2018.09.013

The $\text{Mg}_3\text{Al}_{1-x}\text{Nd}_x$ layered double hydroxides (LDHs) were synthesized *via* aqueous sol–gel synthetic route and the influence of the Nd^{3+} doping on the $\text{Mg}_3\text{Al}_{1-x}\text{Nd}_x$ LDHs properties was estimated for the dopant concentration varied in the range of 1–10 mol%. The microstructure and morphology of the synthesized LDHs were revealed by X-ray diffraction analysis and scanning electron microscopy. The neodymium doped LDHs were characterized by the luminescence emission spectra.



Layered double hydroxides (LDHs) are widely used in commercial products as adsorbents, catalyst support precursors, anion exchangers, acid residue scavengers, flame retardants, osmosis membranes, sensors, *etc.*^{1–6} Considerable attention has been focused on the incorporation of rare earth elements into LDHs host layers in order to develop new functional materials with designed optical properties.^{7–13} The rare earth doped luminescent materials are of increasing interest as potential phosphor materials for applications in optical devices.^{14,15} The organic–inorganic hybrid phosphors have been designed and assembled by the intercalation of organic compounds as sensitizer into the layered lanthanide hydroxides or by changing the doping concentration of the activator ions.^{16–20}

This work was aimed at the fabrication of $\text{Mg}_3\text{Al}_{1-x}\text{Nd}_x$ layered double hydroxides *via* a novel sol–gel method and investigation of effect of Nd^{3+} doping on phase changes, structure and luminescence of the $\text{Mg}_3\text{Al}_{1-x}\text{Nd}_x$ samples. The results revealed the influence of addition of organic ligand on the luminescence of Nd^{3+} in the $\text{Mg}_3\text{Al}_{1-x}\text{Nd}_x$ LDHs.

The $\text{Mg}_3\text{Al}_{1-x}\text{Nd}_x$ LDH samples were synthesised from solutions of $\text{Mg}(\text{NO}_3)_2 \cdot 6\text{H}_2\text{O}$, $\text{Al}(\text{NO}_3)_3 \cdot 9\text{H}_2\text{O}$ (with molar ratio

of 3 : 1), and $\text{Nd}(\text{NO}_3)_3 \cdot 6\text{H}_2\text{O}$.[†] The commercial Mg_3Al LDH (PURAL MG63HT, Brunsbüttel, Germany) was also analyzed as a reference for comparison. The terephthalic acid intercalated $\text{Mg}_3\text{Al}_{1-x}\text{Nd}_x$ hybrid inorganic–organic specimens were prepared by anion exchange method.[‡]

The XRD patterns[§] of $\text{Mg}_3\text{Al}_{1-x}\text{Nd}_x$ ($x = 1–10$ mol%) LDHs synthesized by sol–gel method are shown in Figure 1. Three basal reflections typical of an LDH structure were observed at 2θ of about 11.5° (003), 23° (006), and 35° (009). In addition, two characteristic LDH peaks are clearly seen at about 60.2° and 61.5° , which correspond to the reflections from the (110) and (113) planes. However, the XRD patterns of the $\text{Mg}_3\text{Al}_{1-x}\text{Nd}_x$ sample with $x = 5$ mol% also exhibited reflections of $\text{Nd}(\text{OH})_3$ phase. According to Figure 1, the growth of amount of neodymium causes a monotonic increase in the intensity of these diffraction peaks. Meantime, the XRD patterns of the Mg–Al–Nd–O precursor gels calcined at 650°C (Figure 2) showed the formation of only high crystalline mixed-metal oxides (MMO) without any formation of even traces of separate neodymium oxide phase.

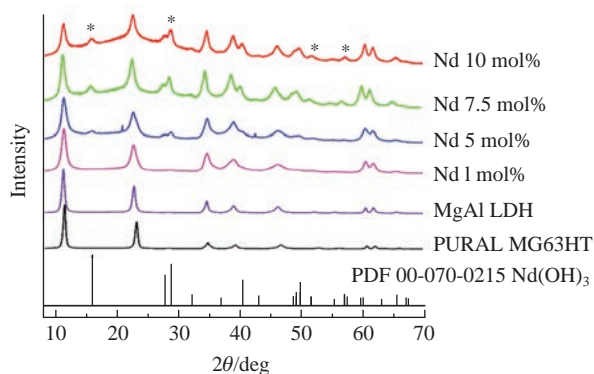


Figure 1 XRD patterns of $\text{Mg}_3\text{Al}_{1-x}\text{Nd}_x$ ($x = 1–10$ mol%) LDHs synthesized *via* sol–gel method and standard XRD patterns of Mg_3Al LDH and $\text{Nd}(\text{OH})_3$. The $\text{Nd}(\text{OH})_3$ phase is denoted by asterisks.

[†] $\text{Mg}(\text{NO}_3)_2 \cdot 6\text{H}_2\text{O}$ (7.69 g, 0.03 mol), $\text{Al}(\text{NO}_3)_3 \cdot 9\text{H}_2\text{O}$ (3.75 g, 0.01 mol), and $\text{Nd}(\text{NO}_3)_3 \cdot 6\text{H}_2\text{O}$ (0.044–0.44 g, 1–10 mmol) were dissolved in distilled water (50 ml), then a citric acid solution (0.2 M, 50 ml) was added and the mixture was stirred at 80°C for 1 h. Ethylene glycol (2 ml) was added to the resulted mixture with continuous stirring at 150°C until the complete evaporation of solvent. The obtained gels were dried at 105°C for 24 h. The mixed metal oxides (MMO) (yields 88%) were obtained by calcination of the gels at 650°C for 4 h. The $\text{Mg}_3\text{Al}_{1-x}\text{Nd}_x$ LDHs were obtained by reconstruction of MMO powders (2 g) in water (150 ml) under stirring at 50°C for 6 h.

[‡] $\text{Mg}_3\text{Al}_{1-x}\text{Nd}_x$ powders (2 mmol) were dispersed in a solution of disodium terephthalate (1.5-fold molar excess) and the mixture was stirred at ambient temperature for 24 h. The solid product was isolated by filtration, washed thoroughly with deionised water and acetone, and dried in oven at 40°C for 12 h.

[§] The X-ray diffraction (XRD) patterns were recorded using a MiniFlex II diffractometer (Rigaku) in $\text{CuK}\alpha$ radiation in the 2θ range from 8 to 80° (step of 0.02°) with the exposition time of 0.4 s per step.

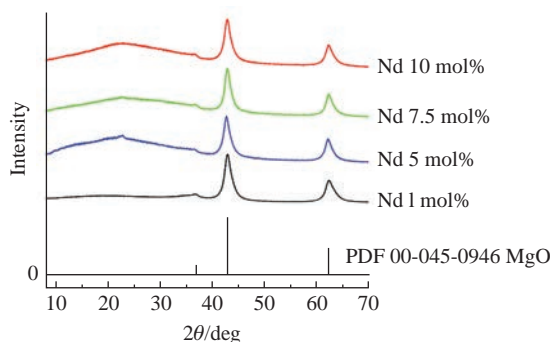


Figure 2 XRD patterns of $\text{Mg}_3\text{Al}_{1-x}\text{Nd}_x$ ($x = 1\text{--}10$ mol%) gels calcinated at 650°C and the standard XRD pattern of MgO .

The formation of plate-like particles with hexagonal shape is well known as the characteristic morphological feature of LDHs.^{21,22} Figure 3 shows the representative SEM micrographs[¶] of $\text{Mg}_3\text{Al}_{1-x}\text{Nd}_x$ ($x = 10$ mol%) and $\text{Mg}_3\text{Al}_{1-x}\text{Nd}_x$ ($x = 5$ mol%) LDH powders synthesized by sol–gel method. The microstructure typical of the LDH was confirmed by these SEM micrographs. The $\text{Mg}_3\text{Al}_{1-x}\text{Nd}_x$ LDHs consist of the hexagonally shaped particles varying in size from approximately 100 to 150 nm. The formation of cloud-like agglomerates from these nanoparticles was also observed.

The luminescent properties of the obtained $\text{Mg}_3\text{Al}_{1-x}\text{Nd}_x$ LDHs were investigated. Unfortunately, these layered double hydroxides as prepared did not demonstrate any luminescence. The attempt to generate the luminescence by intercalating disodium terephthalate in these LDH samples was made. The emission spectra^{††} of $\text{Mg}_3\text{Al}_{1-x}\text{Nd}_x$ LDH samples with terephthalate (TAL) in the interlayer spacing under excitation at 580 nm are shown in Figure 4. The spectra contain several bands located at 900 and 1065 nm, which arise due to the $^4\text{F}_{3/2} \rightarrow ^4\text{I}_{9/2}$ and $^4\text{F}_{3/2} \rightarrow ^4\text{I}_{11/2}$ transitions of Nd^{3+} . Bands near 1165 nm are assigned to the $^4\text{F}_{3/2} \rightarrow ^4\text{I}_{13/2}$ transitions of Nd^{3+} . The intensity of all bands increases proportionally with raising the doping level of neodymium (see Figure 4). The photoluminescence intensity of the $\text{Mg}_3\text{Al}_{1-x}\text{Nd}_x$ LDH phase reaches its maximum at the Nd^{3+} concentration of 7.5 mol%. A further growth of the neodymium amount leads to a slight decrease in the emission intensity due to the concentration quenching.

In conclusion, we accomplished the synthesis of $\text{Mg}_3\text{Al}_{1-x}\text{Nd}_x$ LDHs within the substitution range of lanthanide from 1 to 10 mol% *via* the sol–gel processing route. The XRD analysis results confirmed the formation of monophasic $\text{Mg}_3\text{Al}_{1-x}\text{Nd}_x$ LDHs. Only at higher concentrations of lanthanide (> 5 mol%), the synthesized samples contained also $\text{Nd}(\text{OH})_3$ phase as the impurity. The sol–gel derived $\text{Mg}/\text{Al}_{1-x}\text{Nd}_x$ LDHs consisted of the hexagonally shaped particles varying in size from ~100 to

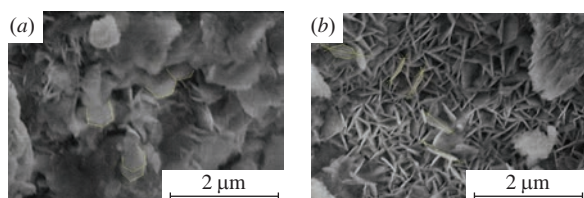


Figure 3 SEM micrographs of $\text{Mg}_3\text{Al}_{1-x}\text{Nd}_x$ LDHs synthesized *via* sol–gel method; (a) $x = 5$ mol% and (b) $x = 10$ mol%.

[¶] The morphology of the LDH powders was analyzed using a Hitachi SU-70 scanning electron microscope (SEM). The particle size was calculated using the ImageJ program.

^{††} The excitation and emission spectra were recorded on an Edinburg Instruments FLS 900 spectrometer.

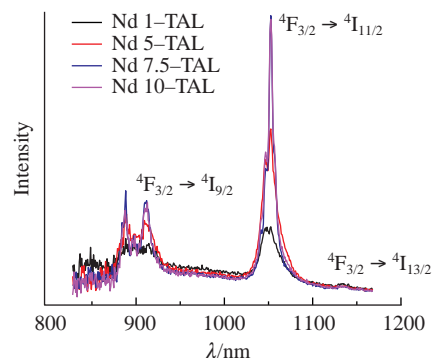


Figure 4 Photoluminescence emission spectra of $\text{Mg}_3\text{Al}_{1-x}\text{Nd}_x\text{-TAL}$ LDHs ($\lambda_{\text{ex}} = 580$ nm).

150 nm. The $\text{Mg}_3\text{Al}_{1-x}\text{Nd}_x$ with terephthalate in the interlayer spacing exhibited the luminescence at 900 nm and 1065 nm, which arose due to the $^4\text{F}_{3/2} \rightarrow ^4\text{I}_{9/2}$ and $^4\text{F}_{3/2} \rightarrow ^4\text{I}_{11/2}$ transitions of Nd^{3+} .

This work was supported by the Research Council of Lithuania (grant SINALAN, no. S-LU-18-13) and by the European Union's Horizon 2020 research and innovation programme (Marie Skłodowska-Curie grant agreement no. 645660) and also partially performed within the framework of the project TUMOCS.

References

- 1 *Advances in Non-Radiative Processes in Solids*, ed. B. di Bartolo, Plenum Press, New York, 1991.
- 2 M. Ivanov, K. Klemkaite, A. Khinsky, A. Kareiva and J. Banys, *Ferroelectrics*, 2011, **417**, 136.
- 3 A. N. Salak, J. Tedim, A. I. Kuznetsova, J. L. Ribeiro, L. G. Vieira, M. L. Zheludkevich and M. G. S. Ferreira, *Chem. Phys.*, 2012, **397**, 102.
- 4 M. Serdechnova, A. N. Salak, F. S. Barbosa, D. E. L. Vieira, J. Tedim, M. L. Zheludkevich and M. G. S. Ferreira, *J. Solid State Chem.*, 2016, **233**, 158.
- 5 P. Lu, S. Liang, L. Qiu, Y. Gao and Q. Wang, *J. Membr. Sci.*, 2016, **504**, 196.
- 6 H. Li, X. Su, C. Bai, Y. Xu, Z. Pei and S. Sun, *Sens. Actuators B*, 2016, **225**, 109.
- 7 K. Binnemans, *Chem. Rev.*, 2009, **109**, 4283.
- 8 P. Gunawan and R. Xu, *J. Phys. Chem. C*, 2009, **113**, 17206.
- 9 P. Vicente, M. E. Pérez-Bernal, R. J. Ruano-Casero, D. Ananias, P. A. A. Paz, J. Rocha and V. Rives, *Microporous Mesoporous Mater.*, 2016, **226**, 209.
- 10 T. Posati, F. Costantino, L. Latterini, M. Nocchetti, M. Paolantoni and L. Tarpani, *Inorg. Chem.*, 2012, **51**, 13229.
- 11 M. Dominguez, M. E. Pérez-Bernal, R. J. Ruano-Casero, C. Barriga, V. Rives, R. A. S. Ferreira, L. D. Carlos and J. Rocha, *Chem. Mater.*, 2011, **23**, 1993.
- 12 Z. Zhang, G. Chen and J. Liu, *RSC Adv.*, 2014, **4**, 7991.
- 13 X. Gao, L. Lei, L. Kang, Y. Wang, Y. Lian and K. Jiang, *J. Alloys Compd.*, 2014, **585**, 703.
- 14 R. Skaudzius, T. Jüstel and A. Kareiva, *Mater. Chem. Phys.*, 2016, **170**, 229.
- 15 A. Stanulis, A. Katelnikovas, D. Ensling, D. Dutczak, S. Sakirzanovas, M. Van Bael, A. Hardy, A. Kareiva and T. Jüstel, *Opt. Mater.*, 2014, **36**, 1146.
- 16 S. Yi, Z. H. Yang, S. W. Wang, D. R. Liu, S. Q. Wang, Q. Y. Liu and W. W. Chi, *J. Appl. Polym. Sci.*, 2011, **119**, 2620.
- 17 D. R. M. Vargas, M. J. Oviedo, F. D. Lisboa, F. Wypych and G. A. Hirata, *J. Nanomater.*, 2013, **153**, 730.
- 18 L. L. Liu, D. Xia, W. S. Liu and Y. Tang, *Chin. J. Inorg. Chem.*, 2013, **29**, 1663.
- 19 A. H. Tamboli, A. R. Jadhav, W.-J. Chung and H. Kim, *Energy*, 2015, **93**, 955.
- 20 W. J. Zhang, Y. L. Li and H. X. Fan, *Opt. Mater.*, 2016, **51**, 78.
- 21 F. R. Costa, A. Leuteritz, U. Wagenknecht, D. Jehnichen, L. Häussler and G. Heinrich, *Appl. Clay Sci.*, 2008, **38**, 153.
- 22 A. Fahami, F. S. Al-Hazmi, A. A. Al-Ghamdi, W. E. Mahmoud and G. W. Beall, *J. Alloys Compd.*, 2016, **683**, 100.

Received: 26th March 2018; Com. 18/5522